Contribution of interface capacitance to the electric-field breakdown in thin-film Al–AlO_x–Al capacitors

Guneeta Singh-Bhalla, Xu Du, and Arthur F. Hebard[a)]
Department of Physics, University of Florida, Box 118440, Gainesville, Florida 32611-8440

(Received 6 June 2003; accepted 5 August 2003)

We present a systematic study of the dependence of breakdown voltages on oxide thickness d in Al–AlO_x–Al thin-film capacitor structures. For sufficiently thin dielectrics, we find that a significant portion of the measured breakdown potential V_b occurs across the electrode interfaces, thereby leading to an overestimate (V_b/d) of the true breakdown electric field E_b across the dielectric. By modeling this interface contribution as an ''interface'' capacitance in series with the geometric ''bulk'' capacitance, we find for high-quality rf magnetron-sputtered AlO_x dielectrics that E_b is independent of d over the range 30–300 Å. © *2003 American Institute of Physics.*
[DOI: 10.1063/1.1613802]

Desirable characteristics for thin-film dielectrics include low leakage currents, high electric field breakdown strength, and a low density of pinholes and interface traps. One particularly popular material satisfying these criteria is amorphous aluminum oxide (AlO_x). For example, thin Al films are found to wet magnetic transition metal alloys, and, when oxidized to completion, form high quality tunnel barriers that promise to be useful in spintronic[1] and magnetic tunnel junction applications.[2,3] Since Al layers more than a few nanometers thick cannot be oxidized to completion, this technique is useful only for tunnel barriers. However, thicker AlO_x can be anodized using Al as the base electrode,[4,5] or grown to a specified thickness by atomic layer deposition[6] or by sputtering techniques.[7–9] Such films have been successfully used for thickness-dependent capacitance studies,[4,7,8] characterization of metal–AlO_x–silicon capacitors,[9] and for field-effect gating of conducting oxides[5] and superconductors.[10,11]

In this letter we present a systematic study of the electric field breakdown in Al–AlO_x–Al trilayer structures where the insulating AlO_x dielectric has a stoichiometry close to that of Al_2O_3 and is deposited to different thicknesses with 5% accuracy in the range 30–300 Å using rf magnetron sputtering of an aluminum oxide target. The most straightforward estimate of the electric-field breakdown strength E_b and the associated maximum areal charge density σ_b is obtained by dividing the measured potential V_m at breakdown ($V_m = V_b$) by the known thickness d, i.e., $E_b = V_b/d$. Assuming that the entire voltage drop is across the dielectric, this corresponds to a surface charge density on the aluminum electrodes at breakdown given by

$$\sigma_b^d = \kappa\epsilon_0 E_b = \kappa\epsilon_0 V_b/d, \tag{1}$$

where κ is the relative permittivity of the dielectric, ϵ_0 is the vacuum permittivity, and the superscript d reminds us that the estimate is made using the dielectric thickness. This procedure, however, must be used with caution, especially for thin dielectrics, because it ignores the voltage drops associated with the presence of interface states and/or the screening of electronic charge at electrode interfaces, thus overestimating the true breakdown potential. We show that this discrepancy can be remedied by using the measured capacitance C_m to calculate the charge $Q_b = C_m V_b$ on the electrodes at breakdown. Thus, for electrodes with area A, the true surface charge density is given by

$$\sigma_b = \sigma_b^Q = C_m V_b/A. \tag{2}$$

Here the superscript Q reminds us that a capacitance measurement is used to measure the charge Q on the electrodes. The discrepancy between σ_b^d and σ_b^Q ($\sigma_b^d > \sigma_b^Q$) can be quantitatively accounted for by modeling the voltage drop across the electrodes as the sum of the voltage drops V_g and V_i, respectively, across a geometrical bulk capacitance C_g connected in series with an interface capacitance C_i (see Fig. 3 inset). Accordingly, the use of Eq. (2) rather than Eq. (1) not only gives the correct value of the maximum surface charge density σ_b that can be obtained near breakdown but also shows in a convincing manner that σ_b^Q is independent of d over the 30–300 Å range studied.

In modeling C_i as a capacitor in series with C_g, the measured capacitance should obey an equation of the form $A/C_m = A/C_i + A/C_g = A/C_i + d/\epsilon_0\kappa$. Accordingly, a plot of the reciprocal areal capacitance A/C_m vs d will exhibit linear behavior with two fitting parameters: an intercept at $d=0$, which determines the value of A/C_i, and a zero crossing at $d=-d_0$ on the negative d axis, which determines the effective plate separation d_0 below which C_i dominates over C_g. For thin film Al–AlO_x–Al trilayers in which the AlO_x was deposited using a dual-gun reactive ion beam sputtering technique, the values $C_i = \kappa\epsilon_0 A/d_0 = 1.62\ \mu\text{F/cm}^2$ and $d_0 = 50$ Å were found.[8] We note that to first order d_0 is independent of κ, since it can be modeled as the product of κ and the sum of the respective screening lengths of both electrodes.[12] Using the series capacitance model, one immediately recognizes that the series combination of C_i and C_g acts as a voltage divider (see inset to Fig. 3) and that the voltage, $V_g = V_m C_i/(C_i + C_g)$, across the bulk dielectric is thus less than the measured voltage V_m. Calculating directly the true charge density $\sigma_b = \kappa\epsilon_0 V_g/d$ at breakdown ($E_b = V_g/d$) across the geometric capacitance, we find the result,

a)Author to whom correspondence should be addressed; electronic mail: afh@phys.ufl.edu

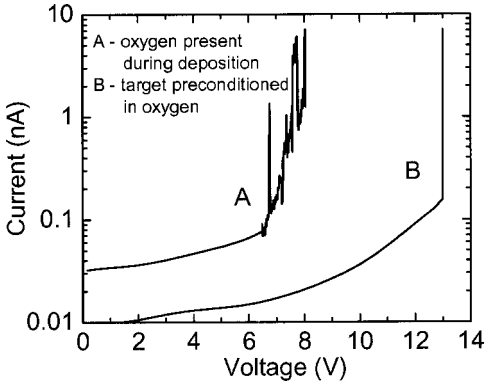

FIG. 1. Current–voltage characteristics at room temperature of two Al–AlO_x–Al capacitors with 300-Å-thick barriers. Trace A (method 3) corresponds to rf sputter deposition with a partial pressure of oxygen in the chamber during deposition. In trace B (method 2) the target has been preconditioned in an oxygen plasma prior to deposition.

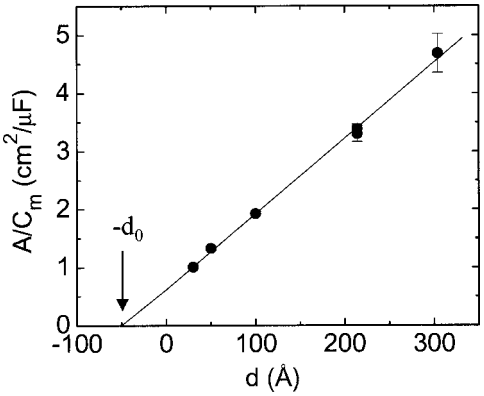

FIG. 2. Plot of reciprocal areal capacitance (1 kHz measurement frequency) as a function of dielectric thickness for the samples deposited using method 1. The linear dependence with nonzero intercept on the ordinate and extrapolation to an effective crossover thickness at $d=-d_0$ (vertical arrow) reflects the presence of a series-connected interface capacitance.

$\sigma_b=\sigma_b^Q=C_mV_b/A$, to be in agreement with Eq. (2). Accordingly, it is necessary to make a capacitance measurement to obtain the correct value of σ_b and the associated breakdown field E_b. These effects have been overlooked in previous studies of thin-film dielectric breakdown in AlO_x films.[6,9,13,14]

For all dielectric depositions the argon pressure was regulated at a pressure of 3 mTorr, well above the system base pressure of 1.5×10^{-8} Torr. The oxides were typically sputtered (rf power at 30 W) at a rate of 2.5 Å/min onto 5 cm×5 cm oxidized silicon substrates precoated with 60-nm-thick aluminum base electrodes deposited using thermal sublimation in a separate chamber. A quartz crystal monitor, calibrated using atomic force microscopy, was used to measure the dielectric thickness. Substrate rotation at approximately one revolution per minute was found to reduce current leakage and increase breakdown strength. The Al counter electrodes were thermally evaporated through a 3 mm diameter circular aperture to a thickness of 60 nm.

Oxides sputtered using three different deposition techniques were compared. The first method (method 1) involved sputtering the oxide target in a 3 mTorr Ar environment. The second method (method 2), with identical deposition parameters, included a 30 min pregrowth target-conditioning step in an additional 3 mTorr O_2 partial pressure. Samples were introduced into the chamber through an evacuated load-lock after conditioning the target. This procedure prevented exposure of the conditioned target to atmospheric gases. Method 3 involved sputtering the oxide with oxygen present in the chamber during deposition. For each of the different deposition methods, four samples measured at each thickness contribute to the error bars in the data gathered.

Figure 1 depicts typical $I-V$ curves of two 300-Å-thick barriers, one sputtered with oxygen present in the chamber (method 3) and the other sputtered from a conditioned target (method 2). Since E_b can depend on the bias voltage ramp speed,[15] consistency between measurements was maintained by using the same ramp rate of 10 V/h for all measurements. Dielectric breakdown is defined to be the point at which the $I-V$ curves become noticeably nonlinear and irreversible. For the data in Fig. 1, this corresponds to approximately 13 V for the conditioned case (method 2) and 6.4 V for the sample grown with oxygen in the chamber (method 3). For all thicknesses measured, the oxides deposited with O_2 present in the chamber have larger leakage currents and significantly lower breakdown strength when compared to the oxides deposited in a pure argon ambient using a conditioned target. Samples grown employing method 1 (unconditioned target and no oxygen present during deposition) exhibit $I-V$ characteristics similar to those depicted for method 2, with the exception of a systematically lower breakdown voltage.

Figure 2 depicts the dependence of A/C_m on d for the Al–AlO_x–Al samples grown using method 1. From the regression fit to the linear dependence, the extracted parameters, C_i/A, κ, and d_0 shown in Table I are in good agreement with previously published results on ion-beam sputtered AlO_x.[8] Similar results for barriers formed using methods 2 and 3 are also shown in Table I. For the method 3 dielectrics, the systematically larger value of d_0 reflects a more diffuse interface, a result consistent with the higher leakage currents and lower breakdown voltages observed for these dielectrics.

Using the series capacitance model together with Eqs. (1) and (2), it is straightforward to show that the ratio of the experimentally determined surface charge densities, σ_b^d and σ_b^Q, gives the dependence, $\sigma_b^d/\sigma_b^Q=1+C_g/C_i=1+d_0/d$. Plots of σ_b^d/σ_b^Q-1 vs $1/d$ for the breakdown measurements obtained for samples made by each method do indeed show this predicted linear dependence with intercepts at the origin and slopes that are equal to the crossover thickness, d_0, as previously defined for the capacitance measurements. As seen in Table I, the slopes of the regression fit to these data for each method give values for d_0 that are within error of

TABLE I. Interface capacitance model parameters extracted from the capacitance and breakdown measurements for each of the three deposition methods.

	Capacitance measurements			Breakdown measurements
Method	κ	C_i/A (μF/cm^2)	d_0 (Å)	d_0 (Å)
1	8.68±0.15	1.62±0.03	47.5±1.4	49.5±1.6
2	8.41±0.16	1.63±0.12	45.8±3.4	47.5±1.0
3	8.43±0.19	1.34±0.03	56.0±1.7	59.7±1.5

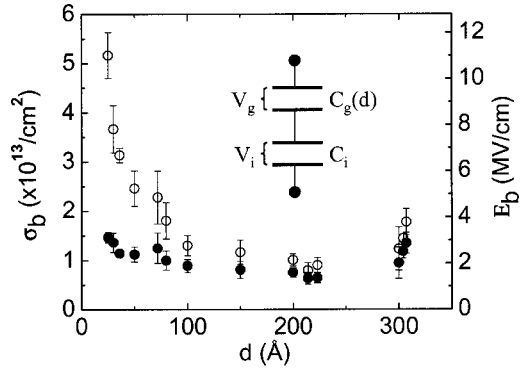

FIG. 3. Plot of σ_b^d (open circles) and σ_b^Q (solid circles) and corresponding breakdown fields (right hand axis) as a function of dielectric thickness d. The true surface charge density σ_b^Q is seen to be approximately constant and independent of thickness. A schematic of the series capacitance model is shown in the inset.

the values obtained using the capacitance measurements (Fig. 2), thus providing a consistency check of the series capacitance model.

Shown in Fig. 3 is the thickness dependence of σ_b^d (open circles) and σ_b^Q (solid circles) as calculated from Eqs. (1) and (2), respectively. The corresponding breakdown field, calculated by multiplying the charge density by $1/\kappa\epsilon_0$, is plotted on the right-hand axis. Use of the series capacitance model corrects for the erroneous divergence of σ_b^d at small d (open circles) and reveals that the true charge density $\sigma_b = \sigma_b^Q$ (solid circles) is independent of d with an average value near 1.1×10^{13} cm^{-2}. This charge density corresponds to a breakdown field $E_b = 2.1$ MV/cm, well below the higher values near 10 MV/cm reported in the literature[6,9,16–18] and also found in our experiments (Fig. 3, open circles, right-hand axis) using the overestimated values implied by Eq. (1) for the thinnest samples.

Low temperature measurements at liquid nitrogen temperatures (77 K) on a small subset of typical samples provide further evidence for the appropriateness of the interface capacitance model. For a typical capacitor with thickness 100 Å, we observe the measured capacitance C_m to be 10% lower at 77 K than at room temperature, while the breakdown voltage V_b was higher at 77 K compared to room temperature by a slightly higher percentage. The relative increase in breakdown strength, expressed as the ratio $\sigma_b^Q(77\ \mathrm{K})/\sigma_b^Q(300\ \mathrm{K})$, is always observed to be less than the measured relative increase in breakdown voltage, i.e., $V_b(77\ \mathrm{K})/V_b(300\ \mathrm{K})$. In previous work on Al–AlO_x–Al thin-film capacitor structures[8,19] the low frequency dispersion and, hence, the temperature dependence has been shown to arise primarily from the contribution of thermally activated interface states. Thus, with decreasing temperature, thermally activated charge redistributions associated with these interface states become less frequent and most of the measured decrease in C_m is due to a decrease in C_i rather than a decrease in C_g. Since as a consequence of the series capacitance model, $V_g = C_i V_m/(C_i + C_g)$, a decrease in C_i therefore implies a corresponding decrease in V_g. Accordingly, at low temperatures the applied voltage must be increased, as is experimentally observed, in order to reach the same or higher breakdown field measured at higher temperatures. The primary advantage of low-temperature operation is not the relatively small increase in intrinsic breakdown strength but rather the substantial decrease (up to four orders of magnitude near breakdown) in leakage currents.

In conclusion, we have presented recipes for the rf sputter deposition of high quality thin-film AlO_x dielectrics and shown that the voltage drop across a series-connected interface capacitance must be taken into account to avoid overestimating the true breakdown field. Measurements of the breakdown voltage and the capacitance, give consistent results when analyzed using a model employing an interface capacitance connected in series with a geometrical capacitance. Using this model we find that the breakdown field and the corresponding maximum in the induced surface charge density is independent of thickness over the range 30–300 Å. Low temperature operation assures a lower leakage current but does not significantly improve the breakdown field.

The authors are grateful to Pradeep Kumar and John Kelly for insightful comments and a critical reading of the manuscript. This work was supported by NSF DMR-0101856.

[1] V. F. Motsnyi, J. De Boeck, J. Das, W. Van Roy, G. Borghs, E. Goovaerts, and V. I. Safarov, Appl. Phys. Lett. **81**, 265 (2002).
[2] S. S. P. Parkin, K. P. Roche, M. G. Samant, P. M. Rice, R. B. Beyers, R. E. Scheuerlein, E. J. O'Sullivan, S. L. Brown, J. Bucchigano, D. W. Abraham, Y. L. Rooks, M. Rooks, P. L. Trouilloud, R. A. Wanner, and W. J. Gallagher, J. Appl. Phys. **85**, 5828 (1999).
[3] J. W. Freeland, D. J. Keavney, R. Winarski, P. Ryan, J. M. Slaughter, R. W. Dave, and J. Janesky, Phys. Rev. B **67**, 134411 (2003).
[4] T. W. Hickmott, J. Appl. Phys. **89**, 5502 (2001).
[5] E. S. Snow, P. M. Campbell, R. W. Rendell, F. A. Buot, D. Park, C. R. K. Marrian, and R. Magno, Appl. Phys. Lett. **72**, 3071 (1998).
[6] M. D. Groner, J. W. Elam, F. H. Fabreguette, and S. M. George, Thin Solid Films **413**, 186 (2002).
[7] K. H. Gundlach and G. Heldmann, Solid State Commun. **5**, 867 (1967).
[8] A. F. Hebard, S. A. Ajuria, and R. H. Eick, Appl. Phys. Lett. **51**, 1349 (1987).
[9] J. Kolodzey, E. A. Chowdhury, T. N. Adam, Guohua Qui, I. Rau, J. O. Olowolafe, J. S. Suehle, and C. Yuan, IEEE Trans. Electron Devices **47**, 121 (2000).
[10] A. F. Hebard, A. T. Fiory, and R. H. Eick, IEEE Trans. Magn. **Mag-23**, 1279 (1987).
[11] A. T. Fiory and A. F. Hebard, Physica B **135**, 124 (1985).
[12] K. T. McCarthy, S. B. Arnason, and A. F. Hebard, Phys. Rev. Lett. **90**, 117201 (2003).
[13] J. W. McPherson and H. C. Mogul, J. Appl. Phys. **84**, 1513 (1998).
[14] T. W. Hickmott, J. Appl. Phys. **88**, 2805 (2000).
[15] W. Oepts, H. J. Verhagen, W. J. M. de Jonge, and R. Coehoorn, Appl. Phys. Lett. **73**, 2363 (1998).
[16] C. Niu, N. P. Magtoto, and J. A. Kelber, J. Vac. Sci. Technol. B **19**, 1947 (2001).
[17] B. Oliver, Q. He, X. Tang, and J. Nowak, J. Appl. Phys. **91**, 4348 (2002).
[18] J. Schmalhorst, H. Bruckl, M. Justus, A. Thomas, G. Reiss, M. Vieth, G. Gieres, and J. Wecker, J. Appl. Phys. **89**, 586 (2001).
[19] K. T. McCarthy, S. B. Arnason, and A. F. Hebard, Appl. Phys. Lett. **74**, 302 (1999).